J Mater Sci: Mater Electron (2016) 27:1270–1277
DOI 10.1007/s10854-015-3885-3

Doping and thickness variation influence on the structural and sensing properties of NiO film prepared by RF-magnetron sputtering

Ehssan Salah Hassan[1] · Asrar Abdulmunem Saeed[1] · Abdulhussain K. Elttayef[2]

Received: 30 May 2015 / Accepted: 6 October 2015 / Published online: 28 October 2015

Abstract The NiO and NiO–Cu doped films with various Cu contents of 5.68, 10.34, and 14.64 at%. Were deposited on a glass substrate with various thickness 50, 100, and 150 nm by RF-reactive magnetron sputtering technique. The effect of the thickness and the doping on the structural, electrical, and sensory properties of the films was mainly investigated. The X-ray diffraction studies revealed that all the deposited films were of single crystalline nature and exhibited cubic structure with preferential growth along 200 and only NiO peaks appear in the NiO–Cu films and when the thickness increased from 50 to 150 nm, the grain size increases from 24.38 to 25.036 nm. Compositional analysis indicated that Cu content increased in the film as the bonded chips increase in the target surface. The electrical resistivity of the NiO film showed a high electrical resistivity 280 K Ω detected by a four point probe measurement and when the Cu content in the films is 5.68 at%. The ρ value is reduced significantly to 45.9 K Ω as Cu content is increased to 10.34 at%, and it further decreases to 25.3 K Ω when the Cu content further increases to 14.64 at% the resistivity value decrease to 10.45 K Ω. The Hall measurement for all NiO and Cu-doped NiO films shows p-type conduction and reduction in the mobility of charge carrier from 9.67×10^2 to 8.46×10 cm^2/V s, when the concentrations of the charge carriers increase from 4.30×10^{10} to 4.23×10^{13} cm^{-3}. The sensory measurements for NiO and Cu-doped NiO films, show that the 50 nm thickness has the highest sensitivity and response time for the NO_2 gas at the operating temperature 150 °C.

1 Introduction

Metal oxide thin films are considerable interest due to their peculiar electrical properties, stability at high temperature and durability. NiO are p-type semiconductors and are in practical use for electronic devices [1]. Electrochromic display devices [2], hetrojunction solar cells [3], p-type transparent conducting films [4] and functional layer materials for chemical sensors [5]. Nickel oxide (NiO) material exhibits both rhombohedral and cubic structure, but the most prominent structure is cubic structure [6]. Is a candidate for p-type MO materials because hole transport originates from nickel vacancies and/or oxygen interstitials, and its band gap is in the range of 3.6–4.0 eV. Generally, the stoichiometric NiO is an insulator with a high electrical resistivity of 10^{13} Ω cm. However, its resistivity value can be reduced significantly by creating nickel vacancies and forming interstitial oxygen atoms in NiO crystallites [7]. Oxide nanocrystalline semiconductor films such as SnO_2–Cu_2O, SnO_2–WO_3, SnO_2–Fe_2O_3, In_2O_3–Fe_2O_3, NiO–Al_2O_3, TiO_2–WO_3 and SnO_2–Fe_2O_3–PdO [3, 4] are widely spread as gas sensitive materials for gas sensor applications. Among these, NiO is an attractive material for sensor applications due to their excellent durability, electrochemical stability and low materials cost. In addition, adding monovalent atoms can also increase conductivity of NiO. Recently many researchers begin to

✉ Ehssan Salah Hassan
ehsanphysicyan@yahoo.com

Asrar Abdulmunem Saeed
asrarabdulmunim@yahoo.com

Abdulhussain K. Elttayef
aelttayef@yahoo.com

[1] Department of Physics, College of Science, Al-Mustansiriyah University, Baghdad, Iraq

[2] Ministry of Science and Technology, Baghdad, Iraq

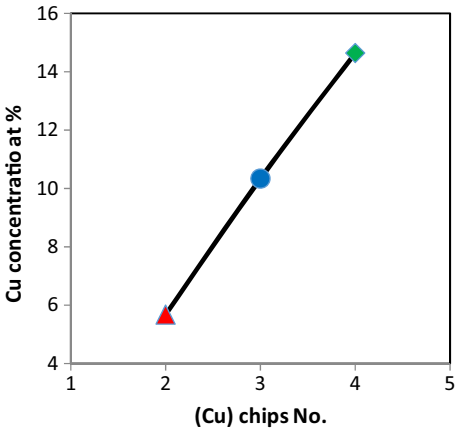

Fig. 1 Copper concentration of NiO:Cu films deposited by RF-reactive Sputtering with various copper concentration

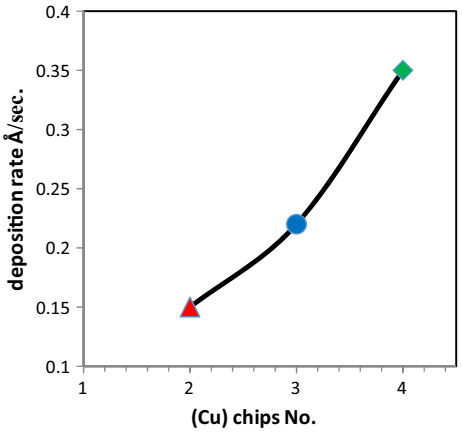

Fig. 3 Deposition rate of NiO:Cu film deposited by RF-reactive Sputtering as function of copper chips bounded to nickel target

tailor the properties of NiO by doping with metal ions. Lung et al. [8] have deposited the lithium doped nickel oxide films with RF magnetron sputtering by varying lithium concentration from 0 to 16 wt%. They observed that the electrical conductivity was decreased at lower concentrations of lithium. Nandy et al. have reported that doping Al atoms into a NiO film enhances the p-type conductivity of the film. Zhao et al. [9] studied that the effect of doping on NiO thin films by means of electrochemical deposition technique. They found that the transmittance value was lowered on Cu doping in NiO films and on further doping, the films exhibited electrochromic behavior. To enhance the electrical properties of the NiO films [10]. There are several methods to fabricate NiO films such as sputtering [11], pulsed laser deposition [12], spray pyrolysis [13], sol–gel [14], vacuum evaporation [15] and atomic layer deposition [16].

2 Experimental

The Cu-doped NiO composite films with 50, 100, 150 nm thickness were deposited on (Superior w. Germany) glass substrates by sputtering NiO–Cu composite targets using radio frequency (RF) magnetron sputtering in both Ar and

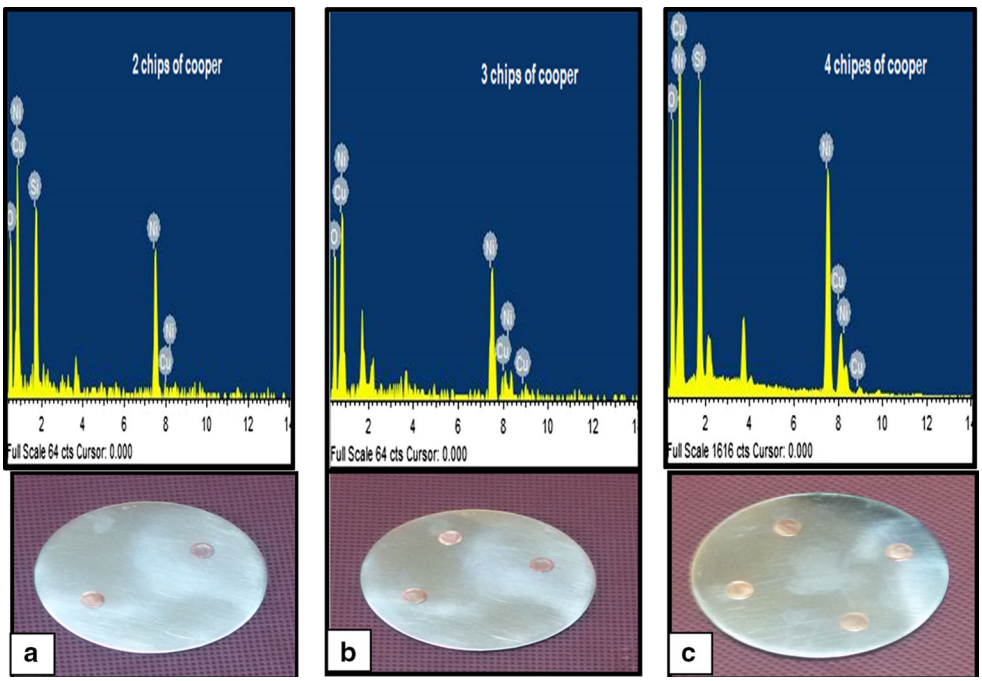

Fig. 2 Energy dispersive spectrometry of NiO:cu deposited by RF reactive magnetron sputtering, **a** two chips of copper doped nickel oxide, **b** three chips of copper doped nickel oxide, **c** four chips of copper doped nickel oxide

Table 1 EDS results for NiO pure and doping NiO:Cu

Cu–Ni–O at% ratios in the NiO in the NiO films			
No. of Cu chips	O	Ni	Cu
2 Cu chips	58.86	35.46	5.68
3 Cu chips	55.47	34.19	10.34
4 Cu chips	53.24	32.12	14.64

O_2 atmosphere. The NiO:Cu composite target comprises of a NiO target (size: 50 mm in diameter, thickness of 3 mm) with varying numbers 2, 3, 4 of bonded Cu cylindrical shape (size: 2.5 mm × 2 mm). The NiO:Cu composite films with Cu contents in the range of 0–14.64 at%. The sputtering powers of the various NiO:Cu composite targets were all set at 200 W. The system has sputter down

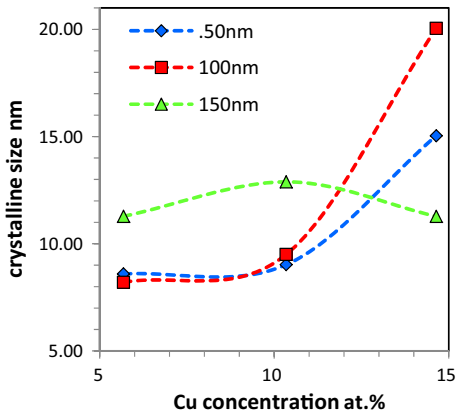

Fig. 6 Crystalline size as function to Cu concentration at% in the NiO films

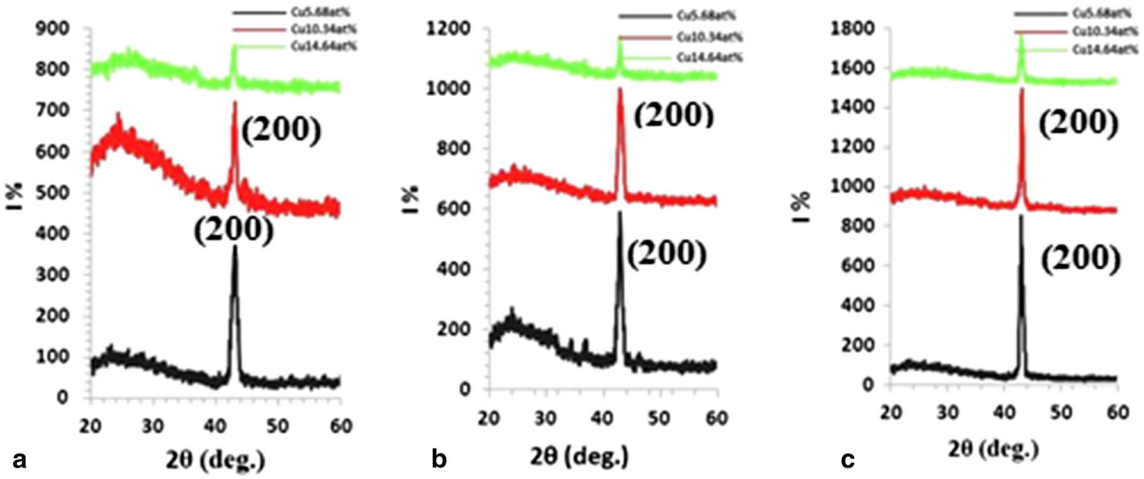

Fig. 4 XRD pattern of nickel oxide doped copper deposited by RF reactive sputtering shows the variation of copper doping with the samples, **a** 50 nm thickness, **b** 100 nm thickness, **c** 150 nm

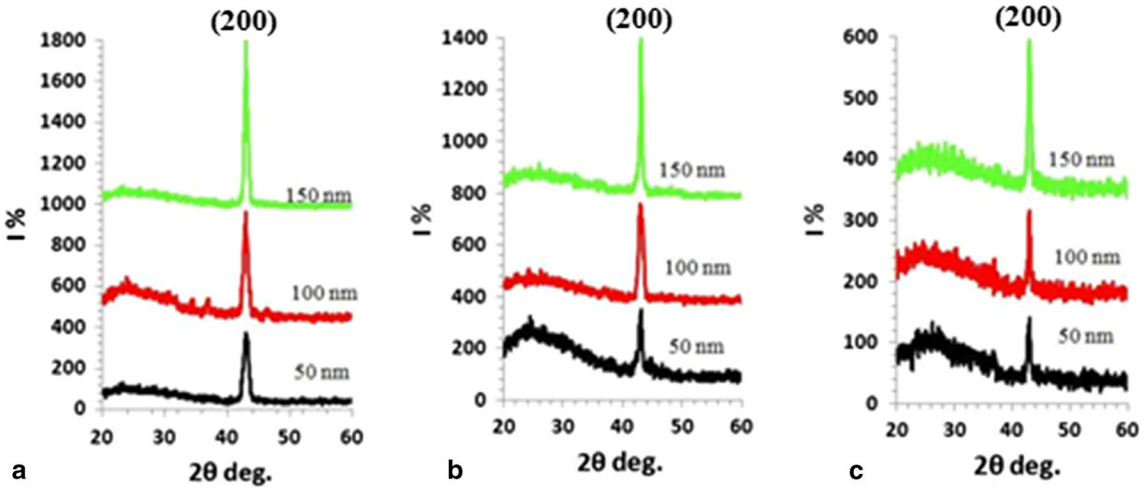

Fig. 5 XRD pattern of nickel oxide doped copper deposited by RF reactive sputtering shows the variation of thickness with the samples, **a** doping by two chips of Cu (5.68 at%), **b** doping by three chips of Cu (10.34 at%), **c** doping by four chips of Cu (14.64 at%)

Table 2 The structural data that valued form XRD pattern for NiO and NiO:Cu samples

Thickness (nm)	(hkl)		FWHM		Crystalline size, L (nm)	
	NiO	NiO:Cu 14.64 at%	NiO	NiO:Cu 14.64 at%	NiO	NiO:Cu 14.64 at%
50	200	200	0.374	0.8	22.894	11.2767
100	200	200	0.350	0.7	24.438	12.8877
150	200	200	0.342	0.6	25.036	15.0367

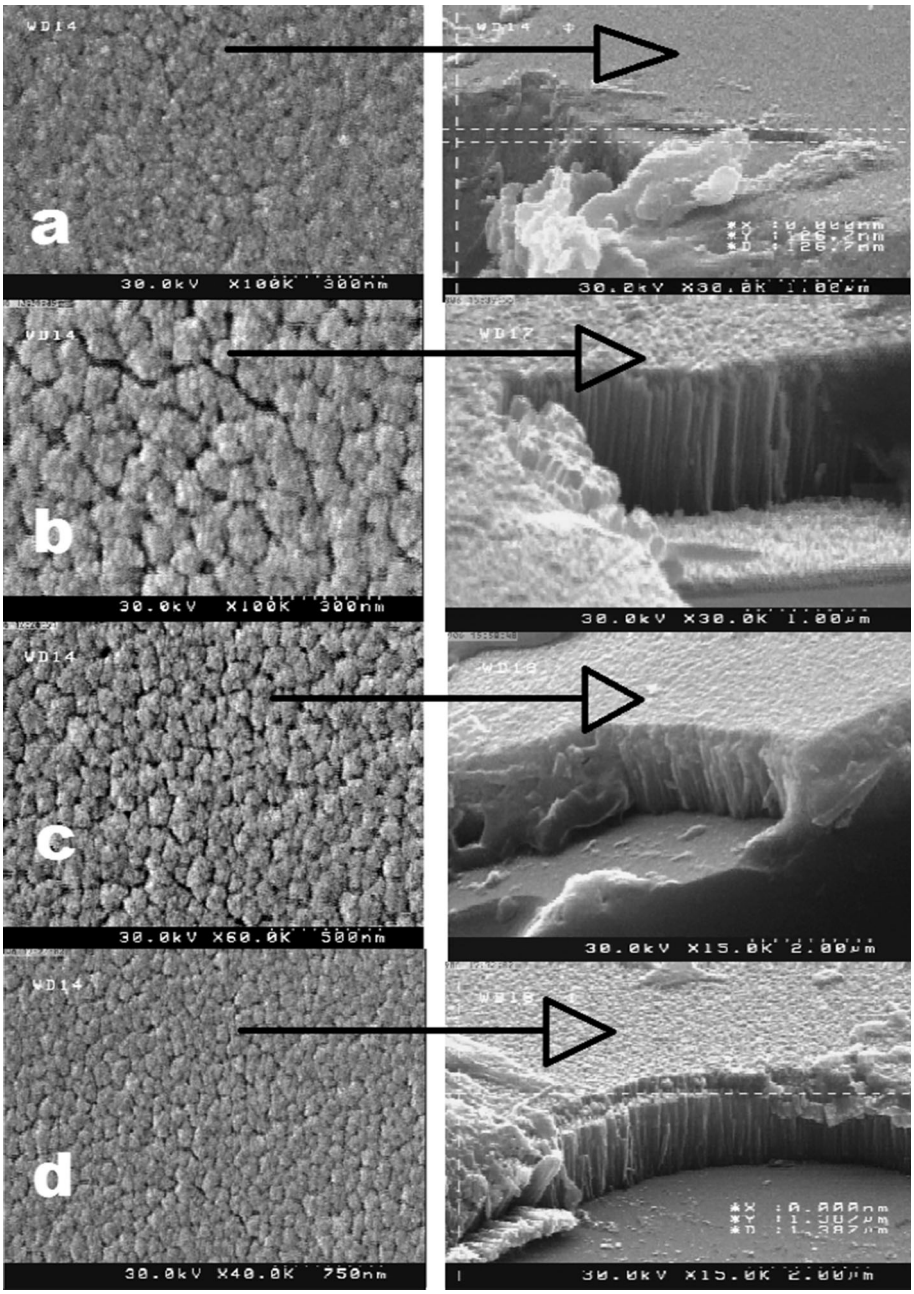

Fig. 7 SEM images of NiO thin films with various copper concentrations. **a** Un-doped, **b** 5.68 at% Cu, **c** 10.34 Cu at%, **d** 14.64 at% Cu

direction. Were the distances and the angel between the target and the substrata is 100 mm and 55° respectively. The deposition rate for the pure NiO film without Cu addition was 0.1 Å/s. It increased to 0.3 Å/s as the number of Cu chips increased to 2, 3 and 4, respectively. The composition ratio of Ni to O in a NiO target of 99.94 %

purity was 1:1 and the purity of Cu chips was 99.99 %. The Ar pressure during deposition of NiO:Cu films was fixed at 1.32×10^{-5} torr. The Sputtering was performed by mixing of Argon and Oxygen gases with pressure approximately 5.62×10^{-2}–1.77×10^{-2} torr respectively. Argon and Oxygen gases penetrate to the chamber with gas mass flue controller (*Ailcat scientific*) the structural properties of the films were analyzed by *XRD* (*shimadzo 6-2006, with cukα radiation having wavelength* $\lambda = 0.15406$ nm). The chemical composition of the films was analyzed by energy dispersive spectroscopy (EDS) attached with SEM of model (*multi-function scanning electron microscope model als 2300 angstrom*). The resistivity, mobility and carrier concentration of the films were measured by using an [*digital multi meter: the PC-interfaced multi meter, of type Proskit* (*MT-1820*). Angstrom]. Electric properties, resistivity, semiconductor type and charge carrier concentration measured by Hall Effect (digital multi meter: the PC-interfaced multi meter, of type Proskit (MT-1820).

3 Result and discussion

Figure 1 shows the contents in NiO:Cu films with varying numbers of Cu chips as measured by EDS. It is found that the Cu content in the films increases almost linearly with the increase number of Cu chips. The Cu content of the NiO:Cu composite target with 2 bonded Cu chips is 5.68 at%. It increases to 10.34 at% as 3 Cu chips are placed on the NiO target. Further increasing the number of Cu chips to 4 the Cu content in NiO–Cu composite films are further increased to 14.64 at%. Figure 2 shows the deposition rate in NiO:Cu films with varying the number of chips as measured by the crystal sensor that attached to the thickness monitor in the RF sputter system. The deposition rate increase with the varying number of the chips due to the higher atomic number of than the nickel [17].

Figure 3 shows elemental composition of the films was determined by EDS and results confirm that all the deposited NiO:Cu films consist of nickel, and oxygen, which is shown in Fig. 3. The composition of the is gradually increased as abounded chips increases. The detailed elemental composition information with respect to atomic percent is listed in Table 1.

Figure 4 shows the XRD patterns of the NiO:Cu composite films with Different Cu contents. All Cu-doped NiO films only display NiO peaks of 200 and Cu peaks do not appear even after adding a higher Cu content into the NiO films. The XRD pattern of NiO:Cu, shows the peak intensity of the NiO:Cu film decreases obviously as Cu content is increased from 5.68 to 14.64 at%. This is due to the substitution of most of the Cu^{+} ions (0.96 Å) for Ni^{+2} (0.78 Å) ions in the NiO lattice, resulting in films widened the 200 peak. This suggests that the doping process of the investigated system brought about an advanced decrease in the degree of crystallinity of NiO phases and led to a progressive decrease in their grain size. The 200 peak shifted towards a low angle as the content increased, which means that the doping process increased the lattice constant of the NiO crystal. Figure 5 show the pure nickel oxide, the peak intensity increases with the film thickness increasing and the X-ray spectra are single crystalline in nature and the crystalline size increase with the thickness increase. Also, the X-ray and electron diffraction patterns indicate that the films deposited on the glass substrates maintained have a NaCl-type structure [18].

Figure 6 shows the variation of crystallite size of NiO:Cu thin films as a function of copper concentration. The increase in the crystallite size may be caused by a columnar grain growth in the structure. The crystallite sizes of pure NiO films were bigger than those deposited with copper doped this suggests that the doping process of the investigated system brought about a progressive decrease

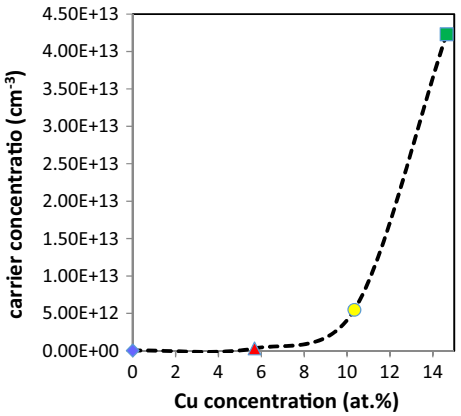

Fig. 8 The variation of carrier concentration as a function to the copper concentration in the NiO films

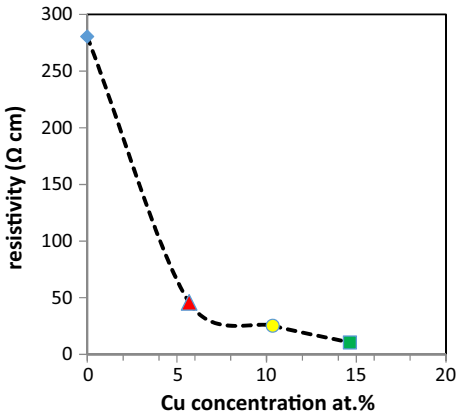

Fig. 9 The resistivity as a function to the copper concentration in the NiO films

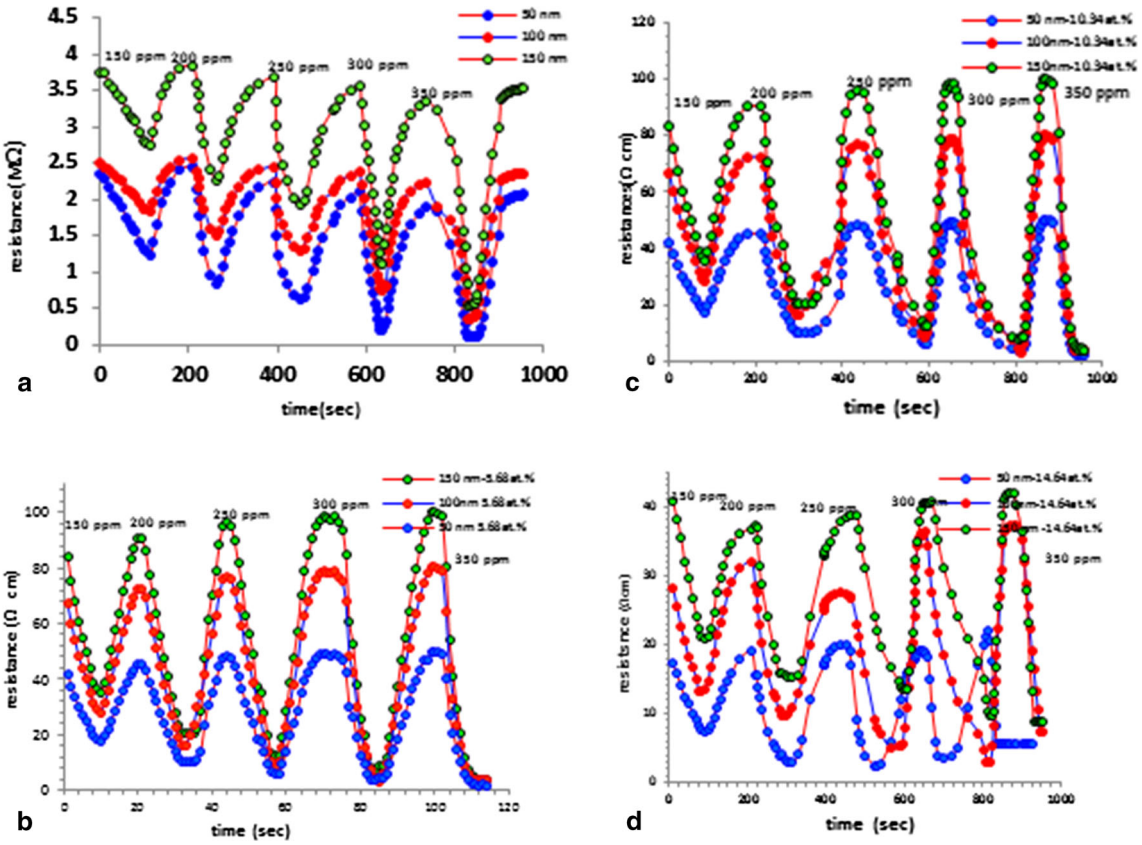

Fig. 10 The variation of resistivity of NO_2 gas with time for **a** as deposited NiO film, **b** NiO:Cu 5.68 at%, **c** NiO:Cu 10.34 at%, **d** NiO:Cu 14.64 at%

in the degree of crystallinity of NiO phases and led to a progressive decrease in their grain size. Table 2 shows the structural data that valued form XRD pattern.

Figure 7 shows the scanning electron microscopy (SEM) images of NiO and NiO:Cu films deposited at different concentration the 50 nm thickness it was observed that very smooth surface and compact surface and the average grain size of abut 50 nm were appeared, and the average grain size was about 60, 70, 75 nm for the 5.86, 10.34, 14.64 at% concentration respectively, the grain size of NiO:Cu films increases progressively graded as the concentration rise and the surface become more rougher.

Figure 8 shows the Hall measurement for the NiO and the Cu-doped NiO films with various contents. We can see that all carrier concentrations are positive for all NiO and concentration in the NiO:Cu composite films exhibit p-type conduction. Furthermore, the carrier concentration is increased from 4.30×10^{10} for NiO film to 4.23×10^{13} for the highest Cu doping concentration 14.64 at% We speculate that large amounts of Ni^{+2} ions in the NiO lattice are replaced by Cu^{+}, which leads to a p-type conduction and an increase in carrier concentration with a subsequent decrease in the ρ value in the NiO–Cu composite film. However, the carrier mobility decreases from 9.67×10^{2} cm^2/V s for NiO film to 8.46×10 cm^2/V s for the highest Cu doping concentration 14.64 at% one possible reason for the decrease in carrier mobility is that fine grains with large amounts of grain boundaries are obtained from NiO–Cu composite films that have a higher Cu content, which would hinder the movement of the carrier. On the other hand, the serious lattice distortion in a Cu-doped NiO film with a higher Cu and from the Eq. (1), we can find the covariant relation between the carrier mobility and the scattering time [19].

$$\mu_p \, \alpha \, \frac{\tau_{sc}}{m^*} \tag{1}$$

where m^* is the effective mass and τ_{sc} is scattering time.

Figure 9 shows the dependence of resistivity (ρ) on the Cu concentration in the NiO:Cu films. The resistivity is seen to decrease from 1.50×10^{5} Ω for NiO to 1.75×10^{3} Ω for the NiO: Cu doped with 14.64 at% at 35 °C temperature it can be explained with the fact that resistivity is known to be inversely proportional to the carrier concentration. The conduction mechanism of the NiO film is believed to be related to the concentration of

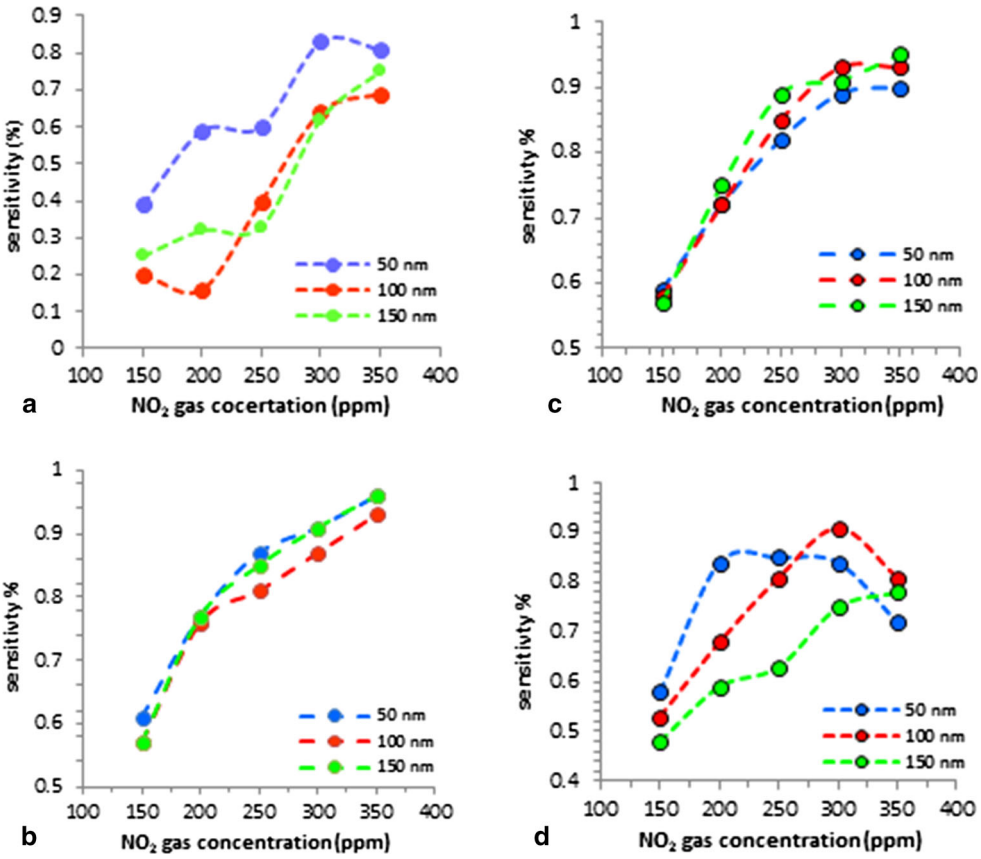

Fig. 11 The sensitivity of NiO films as a function to gas concentration **a** as deposited NiO, **b** NiO:Cu 5.68 at%, **c** NiO: Cu 10.34 at%, **d** NiO: Cu 14.64 at%

the electrical carrier, which is the oxygen vacancy existed in the structure. The electrical properties of NiO films are then associated with their microstructure and composition, and consequently, on the Deposition environment [20].

$$\rho = \frac{1}{ne\mu} \tag{2}$$

where e is the electric charge.

The different thickness 50, 100 and 150 nm of NiO pure and doped with Cu thin films were used in this work as a gas sensor application for nitrogen dioxide (NO_2) gas at various gas concentrations 150–350 ppm with 150 °C operating temperature.

Figure 10 that represents of resistance as a function of response time for different thickness of doped and un-doped films. We observe the resistance decrease of all samples when the nitrogen dioxide gas introduce to the chamber. Which indicate that NiO is p-type semiconductor, which (confirms hall measurement) the oxidizing gases (NO_2), reacts with the film surface, by capture electrons from the conduction band and that increases holes numbers (which represent the majority charge carriers in the p-type semiconductor) in the conduction band, and that leads to decreases the resistance of the film [21]. And generally the resistance (R_g) decreases with Cu concentration increasing in the film. While the increases in the gas concentration from 150 to 350 ppm by 50-ppm step for each case, shows increases in the resistance differ (ΔR) [the difference between the gas resistance in the gas presence (R_g) and gas resistance in the air (R_a)]. And as a result high sensitivity values can be recorded. The sensitivity equation of the oxidation gas with p-type semiconductor is (3).

$$S = \frac{(R_a - R_g)}{(R_a)} \tag{3}$$

The sensitivity of NiO pure and doped with Cu films as shown in Fig. 11, esteemed from the Eq. (3). Figure 11b, c show the sensitivity stable increasing at film doped with 5.68 and 10.34 at%. And when gas concentration increases. The sensitivity values in Fig. 11b found to be 56 % at gas concentration 150 ppm, while increases to 70 % as gas concentration increasing to 200 ppm and increases to 80, 90, 95 % as gas concentration increases up to 300 ppm, respectively. This result can be related to high crystallinity and/or nano crystalline size, which increase the effective area of reaction of the gas with the film surface, also small roughness that indicate high homogeneity of the surface. In addition, high conductivity due to carrier concentration increases. Figure 11d shows increasing in sensitivity with gas concentration increases from 150 to 250 ppm and then

decreases at the gas concentration over 300 and 350 ppm. Witch can be attributed to the same result above.

4 Conclusions

Successful depositing copper-doped nickel oxide nano films with 50, 100, 150 nm thickness by using new technique of bounding chips to the metal target in the RF-reactive magnetron sputtering system. And we can see almost linearly relation between the concentration in the film and the number of the bonded chips on the nickel target surface. The doping played a key role in defining the film properties. The films exhibited better crystallinity and the grain size of the samples increased with increasing concentration in the doped films The resistivity reduced from $1.50 \times 105\ \Omega$ cm for the as deposited NiO to $1.75 \times 103\ \Omega$ cm for the highest concentration 14.64 at% film. The sensitivity of the film of doped with 5.68 at% and the thickness 150 nm shows the best sensitivity of around 95 % at operating temperature 150 °C and for NO_2 gas concentrations at 350 ppm This result can be related to high crystallinity and/or nano crystalline size, which increase the effective area of reaction of the gas with the film surface In addition, high conductivity due to carrier concentration increases. The presence of Cu nanoparticles improved the sensor performance, leading to the detection of NO_2 concentrations at the 350 ppm level. The NiO: Cu sensors were able to operate at 150 °C, which is one of the lowest reported operating temperatures for NiO based nitrogen dioxide sensor.

References

1. N. Barsan, D. Kozieij, U. Weimar, Metal oxide based gas sensor research: how to? Sens. Actuators B **121**, 18–35 (2007)
2. S.J. Ippolito, S. Kandasamy, K. Kalantar-Zadeh, W. Wlodarski, H_2 sensing characterization of WO_3 thin film conductometric sensor activated by Pt and Au catalysts. Sens. Actuators B **108**, 154–158 (2005)
3. C.H. Pandis, N. Brilis, E. Bourithis, D. Tasamakis, Ali H. KrishnamoorathyS et al., Low temperature hydrogen sensor based on Au nanoclusters and Schottky contacted on ZnO films deposited by pulsed laser deposition on Si and SiO_2 substrates. IEEE Sens. J. **7**, 448–454 (2007)
4. R.C. Korošec, P. Bukovec, Sol–gel prepared NiO thin films for electrochromic applications. Acta Chim. Slov. **53**, 136–147 (2006)
5. E. Fujii, A. Tomozawa, H. Torii, R. Takayama, Jpn. J. Appl. **35**, L328–L330 (1996)
6. J. Wang, P. Zhang, J. Qi, P. Yao, Sens. Actuators B Chem. **136**, 399–404 (2009)
7. M. Matsumiya, F. Qiu, W. Shin, N. Izu, N. Murayama, S. Kznzaki, Thin Solid Films **419**, 213–217 (2002)
8. J.W. Lung, L.Y. Ming, H.W. Sing, C.W. Chien, J. Eur. Ceram. Soc. **30**, 503–508 (2010)
9. M. Zhao, X. Wang, L. Ning, J. Jia, X. Li, L. Cao, Electrospun Cu-doped ZnO nanofibers for H_2S sensing. Sens. Actuators B **156**, 588–592 (2011)
10. J. Bandara, C.M. Divarathne, S.D. Nanayakkara, Sol. Energy Mater. Sol. Cells **81**, 429–433 (2004)
11. J.K. Kang, S.W. Rhee, Chemical vapor deposition of nickel oxide films from $Ni(C_5H_5)_2/O_2$. Thin Solid Films **391**, 57–61 (2001)
12. S. Fujihara, C. Sasaki, T. Kimura, Effects of Li and Mg doping on microstructure and properties of sol–gel ZnO thin films. J. Eur. Ceram. Soc. **21**, 2109–2112 (2001)
13. U.S. Joshi, Y. Matsumoto, K. Itaka, M. Sumiya, H. Koinuma, Combinatorial synthesis of Li-doped NiO thin films and their Transparent conducting properties. Appl. Surf. Sci. **252**, 2524–2528 (2006)
14. H. Sato, T. Minami, S. Takata, T. Yamada, Transparent conducting p-type NiO thin films prepared by magnetron sputtering. Thin Solid Films **236**, 27–31 (1993)
15. H. Kumagai, M. Matsomoto, K. Toyoda, M. Obara, Penetration and characteristics of NiO thin film by controlled growth with sequential surface chemical reactions. J. Mater. Sci. Lett. **58**, 1081–1083 (1996)
16. J. Wang, J. Cai, Y.-H. Lin, C.-W. Nan, Room temperature ferromagnetism observed in Fe-doped NiO. Appl. Phys. Lett. **87**, 202501–202503 (2005)
17. P.J. Barth, B. Muller, U. Wagner, A. Bittinger, Quantitative analysis of parenchymal and vascular alteration in NO_2 induced lung injury in rats. Eur. Respir. J. **8**, 1115–1121 (1995)
18. I. Castro-Hurtado, G. Ga Mmandayo, E. Castano, in *Proceeding of the 8th Spanish Conference on Electron Devices CDE*, 2011, 978-1-4244
19. S. Mannan, S.K. De, Magnetic properties of Li and Fe co-doped NiO. Solid State Commun. **149**, 297–300 (2009)
20. L. Zhao, G. Su, W. Liu, L. Cao, J. Wang, Z. Dong, M. Song, Appl. Surf. Sci. **257**, 3974–3979 (2011)
21. A. Bogaerts, R. Gijbels, Behavior of the sputtered copper atoms, ions and excited species in a radio-frequency and direct current glow discharge. Spectrochim. Acta Part B **55**, 279–297 (2000)